Probabilistic soil moisture dynamics of water- and energy-limited ecosystems

Estefanía Muñoz[a,*], Andrés Ochoa[a], Germán Poveda[a], Ignacio Rodríguez-Iturbe[b]

[a] *Universidad Nacional de Colombia, Facultad de Minas, Medellín*
[b] *Texas A&M University, Departments of Ocean Engineering, Civil Engineering, Environmental and Agricultural Engineering, Collage Station, TX 77843*

Abstract

This paper presents an extension of the stochastic ecohydrological model for soil moisture dynamics at a point of Rodríguez-Iturbe et al. (1999) and Laio et al. (2001). In the original model, evapotranspiration is a function of soil moisture and vegetation parameters, so that the model is suitable for water-limited environments. Our extension introduces a dependence on maximum evapotranspiration of available solar radiation, and thus our extended model is suitable for both water- and energy-limited environments. Furthermore, an analysis of the daily relationship between available energy for photosynthesis and transpiration through the stomatal conductance is carried out. This study regards the Penman-Monteith equation to model transpiration, the Leuning's stomatal conductance approach, the C_3 photosynthesis model of Farquhar et al., and the FLUXNET database. Results are upscaled from half-hourly to daily scale, introducing an expression of transpiration in terms of the available radiation. The sensitivity of the model is analyzed using four dimensionless groups, and the long-term water balance is evaluated for distinct values of available energy.

Keywords:
Transpiration, photosynthesis, PAR, stomatal conductance, radiation

*Corresponding author
Email address: emunozh@unal.edu.co (Estefanía Muñoz)

1. Introdution

The soil water content (s) is a key player in the climate-soil-vegetation system (Entekhabi and Brubaker, 1995; Porporato and Rodríguez-iturbe, 2002; Rodríguez-Iturbe and Porporato, 2004). This system involves many variables and processes with high spatial and temporal variability, feedbacks and non-linear relations. Furthermore, soil moisture depends critically on the physiological characteristics of vegetation, pedology and climate (Entekhabi and Rodríguez-Iturbe, 1994; Rodríguez-Iturbe et al., 1999; Rodriguez-Iturbe et al., 2001). Climate and weather patterns determine the amount of water and energy available, crucially impacting the evapotranspiration process (Leuning, 1995; De Pury and Farquhar, 1997; Stoy et al., 2009; Manzoni et al., 2011). Soil texture, its mineralogical composition, and the particle size distribution determine the storage capacity of the soil. Vegetation controls the energy and water fluxes, linking the soil and the atmosphere (Feddes et al., 2001; Rodriguez-Iturbe et al., 2001).

Climate, soil, and vegetation are related through physical, chemical and biological processes, which lead to the mass and energy transport between land and atmosphere (Eagleson, 1978). Actual evapotranspiration couples water and energy balances. There are two evapotranspiration (ET) regimes related to soil moisture, s: an energy-limited regime and a water-limited regime. Between these two regimes, there are seasonal environments, in which the availability of water and energy fluctuates.

Among the approaches to modeling soil moisture are biophysical process-based, physical-based and statistical models (Wang et al., 2019). These models mostly feed on in-situ (e.g. Korres et al., 2015; Noh et al., 2015; Pirone et al., 2015; Gevaert et al., 2018) and remote sensing (e.g. Wagner et al., 1999; Kim and Barros, 2002; Fang and Lakshmi, 2014; Zehe et al., 2018) data or involve numerical simulations (e.g. Mtundu and Koch, 1987; Brubaker, 1995; Brubaker and Entekhabi, 1996; Albertson and Montaldo, 2003; Ridolfi et al., 2003; Rigon et al., 2006; Margulis and Entekhabi, 2001; Sela et al., 2012; Chen et al., 2017; de Assunção et al., 2018). In-situ data are not easy to extrapolate to spatial scales that allow hydrological applications, remote sensing methods measure continuous spatiotemporal information but only comprise the most superficial centimeters of the soil (Niemann, 2004), and numerical simulations do not permit to generalize the results (Ogren, 1993). Daly and Porporato (2005), Seneviratne et al. (2010), Asbjornsen et al. (2011), Legates et al. (2011) and Wang et al. (2019) present some complete reviews of the

state of the art of soil moisture modeling.

Eagleson (1978), Cordova and Bras (1981), Hosking and Clarke (1990), and Milly (1993) initiate a biophysical based approach that comprises simplified but realistic conceptual models that analytically describe the phenomena taking place in the climate-soil-vegetation system. This approach involves stochastic components that take into account the randomness of precipitation and the inherent variability of soil and vegetation properties. Some models have been developed following this approach (e.g. Rodríguez-Iturbe et al., 1999; D'Odorico et al., 2000; Laio et al., 2001; Milly, 2001; Laio et al., 2002; Porporato et al., 2003; D'Odorico and Porporato, 2004; Daly and Porporato, 2006; De Michele et al., 2008; Laio et al., 2009), modeling precipitation as a stochastic process and deriving analytical expressions of soil moisture dynamics from the soil, climate and vegetation parameters. These models have been developed for arid and semi-arid environments, characterized by scarce rainfall, low soil moisture, recurrent water stress, and deep water table (Laio et al., 2009). Since the available energy is not directly considered, they are not suitable to be applied in energy-limited environments.

Photosynthetically active radiation (PAR) is the energy source of biophysical processes, such as photosynthesis, stomatal conductance, transpiration, evaporation, leaf temperature, plant growth, seedling generation, biochemical cycling, and atmospheric chemistry (Thorpe et al., 1978; Baldocchi and Meyers, 1991; Baldocchi and Collineau, 1994; Ballaré, 1994; Hansen, 1999; Yu et al., 2004; Daly et al., 2004; Ge et al., 2011), which are directly or indirectly related to s. On the other hand, the stomata movement regulates simultaneously the water and CO_2 fluxes during transpiration and photosynthesis (Collatz et al., 1991; Yu et al., 2004; Medlyn et al., 2017; Shan et al., 2019), being necessary to model photosynthesis and transpiration coupled with the stomatal conductance (g_s).

In this study, we propose an extension of the model by Rodríguez-Iturbe et al. (1999) and Laio et al. (2001) towards the representation of the stochastic behavior of soil moisture in both water- and energy-limited environments. The moisture loss model proposed by Laio et al. (2001) is modified in such a way that actual ET becomes a function of soil moisture and available radiation. Then, we analyze the relations of transpiration (T) and available radiation, and transpiration and soil moisture when radiation is the limiting variable. Stomatal conductance is modeled using the Leuning's approach (Leuning, 1990, 1995), and transpiration using the Penman-Monteith equation. Net assimilation of CO_2 (A_n) is determined with the Farquhar model

Table 1: Parameters for the stomatal and transpiration models.

Parameter	Value	Description
a_1	18	Eq. 3
c_a [μmol mol^{-1}]	350	Atmospheric CO_2 concentration
c_p [J kg^{-1} K^{-1}]	1013	Specific heat of air
D_x [Pa]	300	Eq. 3
e	0.622	Ratio molecular weight of water vapour/dry air
g_a [mm s^{-1}]	20	Atmospheric conductance
g_b [mm s^{-1}]	20	Leaf boundary layer conductance
LAI [m m^{-1}]	1.4	Leaf area index
λ_w [J kg^{-1}]	$2.26 \cdot 10^6$	Latent heat of water vaporization
ρ_a [kg m^{-3}]	1.2	Air density
ρ_w [kg m^{-3}]	997	Water density

and information from the FLUXNET database. The dependence of g_s and T on available PAR is integrated at the daily level, relating T and PAR through a simple expression. Finally, we analyze the sensitivity of the probability density distribution (pdf) to the available energy and the long-term water balance.

2. Data

Half hourly resolution data of air temperature (T_a), atmospheric pressure (P_a), vapor pressure deficit (Δ_e), photosynthetic photon flux density (PPFD), net ecosystem CO_2 exchange (NEE), CO_2 air concentration, and soil moisture in 28 sites around the world are taken from the FLUXNET dataset (Baldocchi et al., 2001; Olson et al., 2004). NEE data contain positive values during the day (assimilation), and negative values during the night (respiratory loss) (Drake and Read, 1981), therefore the positive values of these series are used as A_n. Table 1 shows the parameters for applying Penman-Monteith and Leuning equations, and Table 2 those for applying the Farquhar model. These values are the same published by Daly et al. (2004).

3. Transpiration dynamics

The major components in the earth's hydrological cycle are transpiration and evaporation. Their analysis and understanding are fundamental

Table 2: Parameters for the C_3 photosynthesis model.

Parameter	Value	Description
H_{Kc} [J mol^{-1}]	59430	Activation energy for K_c
H_{Ko} [J mol^{-1}]	36000	Activation energy for K_o
H_{vV} [J mol^{-1}]	116300	Activation energy for $V_{c,max}$
H_{dV} [J mol^{-1}]	202900	Deactivation energy for $V_{c,max}$
H_{vJ} [J mol^{-1}]	79500	Activation energy for J_{max}
H_{dJ} [J mol^{-1}]	201000	Deactivation energy for J_{max}
J_{max_0} [μmol m^{-2} s^{-1}]	$2 \times V_{c,max0}$	Eq. A.5 (Kattge and Knorr, 2007)
K_{c_0} [μmol mol^{-1}]	302	Michaelis constant for CO_2 at T_0
K_{o_0} [μmol mol^{-1}]	256	Michaelis constant for O_2 at T_0
o_i [mol mol^{-1}]	0.209	Oxygen concentration
R_g [J mol^{-1} K^{-1}]	8.31	Universal gas constant
S_v [J mol^{-1} K^{-1}]	650	Entropy term
T_0 [K]	293.2	Reference temperature
V_{c,max_0} [μmol m^{-2} s^{-1}]	50	Eq. A.3
γ_0 [μmol mol^{-1}]	34.6	CO_2 compensation point at T_0
γ_1 K^{-1}]	0.0451	Eq. 4
γ_2 K^{-2}]	0.000347	Eq. 4

in applications associated with biogeochemical cycles, nutrient losses, salt accumulations of soil, production efficiency, etc. (Schulze et al., 1995). Transpiration couples water and carbon cycles (Miner et al., 2017; Shan et al., 2019), while evapotranspiration couples water and land-surface energy balances (Fisher et al., 2009; Seneviratne et al., 2010; Zhang et al., 2016). These links are driven by vegetation, climate, and soil, existing a close dependence between atmosphere and vegetation. The sensible and latent heat fluxes from vegetation cause changes in the atmosphere state and, at the same time, vegetation responds to changes in air temperature and humidity (Monteith and Unsworth, 2013). Vegetation closes its stomata in the absence of light or water in the soil so that both radiation and soil moisture are variables directly related to transpiration (Monteith, 1995).

Although transpiration (T) responds to a wide variety of complex environmental and physiological factors (Cowan and Farquhar, 1977; Tuzet et al., 2003), here it is assumed that T can be limited by three factors: soil water, energy, and vegetation capacity (physiology) (see Fig. 1). The maximum rate at which vegetation can transpire when it has no external limitations depends on the maximum stomatal conductance, which is directly proportional to pore width (Larcher, 1995). This rate is T_{maxmax} and is represented by the red line in Fig. 1. The left panel of Fig. 1 shows the relationship of transpiration rate and available radiation (R) when there are no water limitations (green line). This relationship is direct until a value of R where transpiration ceases increasing. This dependence is analyzed in detail in section 3.3. The right panel in Fig. 1 indicates the relationship of transpiration and soil moisture. The dark blue line shows the transpiration rate when it is limited by soil moisture and vegetation physiology, but not by energy. Transpiration is maximum for values of s greater than the incipient stomata closure (s^*) (T is equal to T_{maxmax}). For values lower than s^*, T begins to decrease because vegetation closes its stomata to avoid internal losses of water. Transpiration continues to reduce until the wilting point (s_w) where it becomes zero. When considering both water and energy limitations, energy limits transpiration for values above s^* (see the plateau of the right graph in Fig. 1), while soil moisture limits for values below s^* (Petersen et al., 1992).

High values of available energy (R) result in higher maximum transpiration rates (T_{max}). For example, as shown by the light blue lines in Fig. 1, a high available energy value (R_1) derives in a higher transpiration rate for $s > s^*$ (T_{max1}) than a low available energy value (R_2) that results in a lower value of transpiration (T_{max2}). In this case, both T_{max1} and T_{max2} are lower

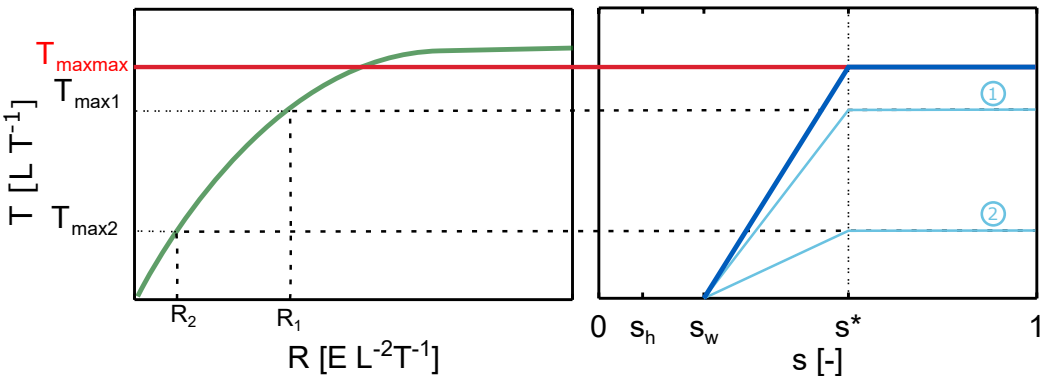

Figure 1: Limitations of transpiration. Left (right) graph illustrates the dependence of transpiration on available energy (water). T_{maxmax} indicates the maximum transpiration rate when there are no external limitations.

than T_{maxmax}, therefore, the plateaus of both light blue lines are determined by the available radiation. Energy also influences the response of the plant to water stress (Petersen et al., 1991, 1992). The rate of water loss is proportional to the water vapor concentration gradient within the vegetation and the bulk atmosphere (Pallardy, 2008), and high radiation values result in high vapor-pressure deficit in the air. When there is much energy in the atmosphere, the vegetation must react more drastically to the water stress ($s < s^*$), because it can lose water at a high rate (see the steeper light blue line 1 from s^* to s_w in the right panel of Fig. 1). Vegetation begins to rapidly close their stomata as soil moisture decreases, reducing its transpiration from T_{max1} when $s > s^*$ to zero when $s < s_w$. On the other hand, when energy demand is low (R_2), vegetation can also suffer water stress, but its reaction may be slighter (Kaufmann, 1976), as shown in the light blue line 2 with T_{max} equal to T_{max2}.

3.1. Water-limited ecosystems

The water-limited regime occurs when ET is very sensitive to s. This regime is associated with arid and semi-arid ecosystems (Budyko, 1974; Eagleson, 1982; Seneviratne et al., 2010). Water restricts ET by its scarcity, intermittency, and unpredictability (Porporato and Rodríguez-iturbe, 2002), and photosynthesis is controlled by soil moisture (Porporato and Rodríguez-iturbe, 2002; Daly et al., 2004).

When soil moisture decreases, vegetation reduces its stomata aperture avoiding changes in its internal water status (Cowan and Farquhar, 1977;

Lhomme, 2001). Stomata close as a response to a signal from the roots when the soil is dry before leaf wilting (Schulze, 1986). This phenomenon is known as vegetation water stress and occurs because vegetation needs an adequate level of humidity in their tissues to growth and survival (Davies et al., 1990; Lhomme, 2001). The description and effects of water stress are widely explained by Schulze (1986); Davies et al. (1990); Flexas and Medrano (2002); Chaves et al. (2003); Xu et al. (2010); Tardieu et al. (2018), among others. Laio et al. (2001) proposed a transpiration model as a function of soil moisture for arid and semi-arid regions. In this model, there are no energy limitations, and it is expressed as:

$$T(s) = \begin{cases} 0, & 0 < s \leq s_w \\ T_{max}\frac{s-s_w}{s^*-s_w}, & s_w < s \leq s^* \\ T_{max}, & s^* < s \leq 1. \end{cases} \quad (1)$$

The term T_{max} represents the maximum evapotranspiration for the vegetation in the presence of unlimited water and energy. When $s < s^*$, T is assumed to decrease linearly because of the limitations of soil moisture until it reaches the wilting point, s_w. Below s_w transpiration ceases. The right panel of Fig.1 represents the behavior of transpiration as modeled by Eq. 1.

3.2. Energy-limited and seasonal ecosystems

The energy-limited regime occurs when soil moisture is most of the time greater than a critical value, with ET weakly dependent on s (Budyko, 1974; Seneviratne et al., 2010). This regime is associated with wet ecosystems. Light limits by its high spatiotemporal variability, that is related to structural and environmental heterogeneity (gapping and clumping of foliage, gaps in the canopy, leaf orientation, type and distribution of clouds, topography, seasonal trends in plant phenology, and seasonality movements of the sun) (Baldocchi and Collineau, 1994).

Radiation in the spectral band of photosynthetically active radiation (PAR) directly drives the fundamental plant physiological processes involving in transpiration, i.e., photosynthesis, stomatal conductance, and leaf temperature. Besides, it indirectly influences secondary processes such as plant growth, seedling generation, structure, and gas emission (Monteith, 1965; Baldocchi and Meyers, 1991; De Pury and Farquhar, 1997).

Transpiration and photosynthesis are processes taking place simultaneously since vegetation loses water through transpiration when take up CO_2 to photosynthesis (Daly et al., 2004; Yu et al., 2004). Photosynthetic rate is

a function of irradiance, CO_2 concentration, temperature, nutrient and, water supply (Luoma, 1997). However, under well-watered conditions, PAR is one of the major environmental factors controlling photosynthesis, stomatal conductance, and consequently, transpiration, in a great number of species (Kaufmann, 1976; Schulze et al., 1995; Mielke et al., 1999; Gao et al., 2002). Stomatal conductance and transpiration increase with PAR (Gao et al., 2002; Pieruschka et al., 2010), as shown in the left graph of Fig. 1. This can be explained by the proportionality between the potassium cation concentration in guard cells and PAR. An increase in the potassium cation concentration causes a decreasing in the osmotic potential of guard cells, resulting in additional water leaves epidermal cells and enter guard cells. This provokes great turgor pressure inside guards and reduces turgor on subsidiary cells so that the vegetation opens its stomata, rising thus its conductance and transpiration (Cooke et al., 1976; Gao et al., 2002; Yu et al., 2004). In seasonal ecosystems, the availability of water and energy fluctuates, and vegetation can present unique adaptations and effects on the hydrological cycle that differ from water and energy limited ecosystems (Asbjornsen et al., 2011).

The expression of transpiration of Laio et al. (2001) manages to describe the daily ET dynamics in energy-limited and seasonal ecosystems provided that E_{max} is defined taking into account the available energy, and stationarity is maintained both in the parameters that describe rainfall and radiation. Fig. 2 represents transpiration as a function of soil moisture and available energy ($T(s, R)$) for a particular set of parameter values. The Penman-Monteith equation is used to relate radiation and T_{max}, varying radiation from 0 to 18 MJ m^{-2} (for a fixed stomatal conductance). This figure shows that when the available radiation is high, the rate at which transpiration decreases with s is much stepper than when radiation is low, representing the response of vegetation to atmospheric demand. We notice that for $R_n = 0$ there is still minimal evapotranspiration due to the non-zero value of the adiabatic term.

3.3. Transpiration and available energy

Available energy affects transpiration, stomatal aperture and photosynthesis through light receptors driving CO_2 fixation and lower intercellular CO_2 concentration (Yu et al., 2004), and determining the diabatic component of transpiration (Monteith and Unsworth, 2013). Hence, to properly study the effects of radiation on transpiration (T), the relations among carbon assimilation (A_n), stomatal conductance (g_s) and transpiration must be

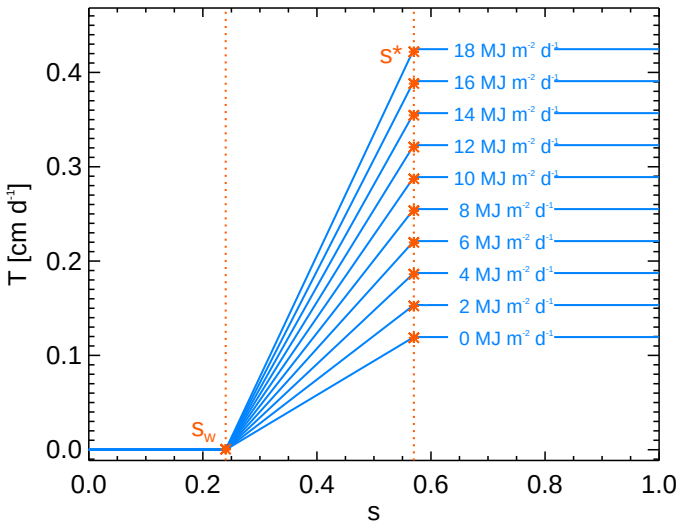

Figure 2: Transpiration as a function of soil moisture and available radiation according to the Penman-Monteith equation and Laio et al. (2001) model. Each horizontal line represents an available radiation value. The parameters used in this figure are $Z_r = 90$ cm, $\lambda = 0.1$ d^{-1}, $\alpha = 1.5$ cm, $\Delta = 0$ cm, $E_w = 0.05$ cm d^{-1}, $E_{max} = 0.43$ cm d^{-1}, $s_h = 0.1$, $s_w = 0.24$, $s^* = 0.57$, $T_{min} = 17.1$ °C, $T_{max} = 28.1$ °C, $r_a = 20.76$ s m^{-1}, $r_c = 69.4$ s m^{-1} and $G = 0$ MJ m^{-2}.

taken into account. For this, the Penman-Monteith equation, the Leuning's stomatal conductance model, the Farquhar model, and a simplified energy balance model are solved numerically and simultaneously. This solution is at a half-hourly scale since the information from the FLUXNET database has this resolution, but as this analysis is carried out to use the Laio et al. (2001) model, these results are integrated on the daily scale. Bartlett et al. (2014), Daly et al. (2004) and Leuning et al. (1995) present methodologies to solve simultaneously stomatal conductance, CO_2 assimilation, and energy balance.

Penman-Monteith equation (Monteith, 1965; Monteith and Unsworth, 2013) is adopted because it is widely used in hydrology, and relates transpiration and stomatal conductance. It is expressed as:

$$T = \frac{\left(\rho_a c_p D g_{ba} + \Delta_e R\right) g_s LAI}{\rho_w \lambda_v \left[\Delta_e g_s LAI + \gamma_p \left(g_{ba} + g_s LAI\right)\right]}, \tag{2}$$

where λ_v is the latent heat of vaporization (2.26 MJ kg^{-1}), ρ_w and ρ_a are the water (998.2 kg m^{-3}) and air (1.2 kg m^{-3}) densities, respectively, c_p is the specific heat of air (1.013·10^{-3} MJ kg^{-1} K^{-1}), Δ_e is the slope of saturation of vapor pressure, γ_p is the psychometric constant, D is the saturation vapor pressure deficit, LAI is the leaf area index, and g_{ba} is the series of leaf boundary conductance (g_b) and atmospheric boundary layer conductance (g_a). Both g_a and g_b are assumed to be constant. The first term in Eq. 2 is the adiabatic component which accounts for the atmospheric saturation deficit, and the second term is the diabatic component of latent heat loss, related to radiation supply. According to the Penman-Monteith equation, T increases linearly with R and with the atmospheric saturation deficit. As g_{ba} is strongly related to wind speed, when it increases, T also increases, and when variables in the numerator remain constant, Δ_e increases with temperature.

3.3.1. Stomatal conductance

Stomatal conductance (g_s) can be calculated using physiological and biochemical models (e.g. Jarvis, 1976; Farquhar et al., 1980; Ball et al., 1987; Farquhar, 1989; Collatz et al., 1991; Leuning, 1995; Gao et al., 2002; Dewar, 2002; Tuzet et al., 2003; Yu et al., 2004). The models most widely used are those based on Jarvis (1976) (e.g. Baldocchi and Meyers, 1991; Peters-Lidard et al., 1997; Daly et al., 2004; Yu et al., 2004) and Ball et al. (1987) (e.g. Leuning, 1990, 1995; Leuning et al., 1995; Daly et al., 2004) approaches.

Net assimilation and transpiration are processes coupled with the stomatal aperture. Therefore, a stomatal conductance model that relates transpiration to net assimilation is necessary to analyze the dynamics of transpiration. For this purpose, we use the semi-empirical formulation given by Ball et al. (1987) and improved by Leuning (1990, 1995), expressed as:

$$g_s = 1.6 a_1 \frac{A_n}{(c_s - \Gamma^*)\left(1 + \frac{D}{Dx}\right)}. \tag{3}$$

This equation gives g_s in terms of carbon assimilation (A_n), water vapor saturation deficit (D), CO_2 compensation point (Γ^*), carbon concentration at the leaf surface (c_s), a fitted parameter representing the sensitivity of stomata to changes in D (D_x), and an empirical constant with a typical value around 15 (a_1). The CO_2 compensation point is the CO_2 concentration at which the CO_2 uptake rate in the photosynthesis equals the CO_2 loss rate of respiration (Birmingham and Colman, 1979). Γ^* is significantly affected by leaf temperature, and according to Brooks and Farquhar (1985), they can be related by:

$$\Gamma^* = \gamma_0 + \left[1 + \gamma_0 (T_l - T_0) + \gamma_2 (T_l - T_0)^2\right], \tag{4}$$

where γ_0, γ_1 and γ_2 are empirical constants, T_0 is the reference temperature, and T_l is the leaf temperature.

3.3.2. Energy balance

Since when solving Eqs. 2 and 3 there are three unknowns (T,g_s and T_l), it is mandatory to couple another equation that allows solving the system, in this case the energy balance equation:

$$T_l = T_a + \frac{R - \rho_w \lambda_w T}{c_p \rho_a g_a}. \tag{5}$$

3.3.3. Net carbon assimilation

The Farquhar model (Farquhar, 1973; Cowan and Farquhar, 1977; Farquhar et al., 1980) is applied to calculate A_n in sites where there are no measurements of it. This is the most frequently used model to quantify the responses of C_3 plants to external perturbations under well-watered conditions. The biochemical demand for CO_2 is determined as a function of the photosynthetic photon flux density (Q), CO_2 concentration in the mesophyll cytosol (c_i) and leaf temperature (T_l), and expressed as:

$$A_n = f\left(Q, c_i, T_l\right) = \min\left[A_c, A_q\right], \tag{6}$$

where A_c and A_q are the photosynthesis rates limited by the Ribulose bisphosphate carboxylase-oxygenase (Rubisco) activity, and by the Ribulose bisphosphate (RuP_2) regeneration through electron transport, respectively (see AppendixA for more details).

3.3.4. Upscaling from half-hourly to daily timescale

The results obtained with the models of transpiration, stomatal conductance, and net assimilation have the temporal resolution of FLUXNET data, i.e, half-hour. To evaluate the daily dynamics of transpiration, we integrate both the calculated results and the information from the FLUXNET database at this time scale. The daily values of s, T and g_s correspond to the average during the day, while PAR and A_n are the cumulative sub-daily values.

4. Soil moisture dynamics

Rodríguez-Iturbe et al. (1999) proposed a daily stochastic zero-dimensional model for soil moisture dynamics at a point in terms of climate-soil-vegetation interactions, under seasonally fixed conditions. The stochastic behavior of rainfall propagates through interception, evapotranspiration, runoff, leakage and soil moisture. Rainfall is modeled as a marked Poisson process that generates infiltration into the soil as a function on the existing soil water content until it reaches saturation. Soil water losses are due to evapotranspiration and leakage, which also depend on the soil moisture state. Soil moisture dynamics is the result of the water mass balance over the plant's rooting depth, expressed by the stochastic differential equation:

$$nZ_r \frac{ds\left(t\right)}{dt} = \varphi\left[s\left(t\right), t\right] - \chi\left[s\left(t\right), R\left(t\right)\right], \tag{7}$$

where n is the soil porosity, Z_r is the rooting depth, s is the soil water content, R is the available radiation, $\varphi\left[s\left(t\right), t\right]$ is the infiltration rate, and $\chi\left[s\left(t\right), R\left(t\right)\right]$ is the soil moisture loss rate.

Infiltration is a stochastic component, expressed as:

$$\varphi\left[s\left(t\right), t\right] = P\left(t\right) - I\left(t\right) - Q\left[s\left(t\right), t\right], \tag{8}$$

where $P\left(t\right)$ is the rainfall rate, $I\left(t\right)$ is the rainfall rate intercepted by the canopy, and $Q\left[s\left(t\right), t\right]$ is the rate of surface runoff generation.

Soil water losses are evaporation, transpiration and, leakage, thus the total water loss rate (χ) is given by:

$$\chi\left[s\left(t\right),R\left(t\right)\right]=ET\left[s\left(t\right),R\left(t\right)\right]+L\left[s\left(t\right)\right], \tag{9}$$

where $ET\left[s\left(t\right),R\left(t\right)\right]$ and $L\left[s\left(t\right)\right]$ are the evapotranspiration and leakage rates, respectively.

ET is modeled as the sum of evaporation (E) and transpiration (T). E is a fixed rate equal to E_w when $s_w \leq s \leq 1$, which decreases from s_w until it reaches the hygroscopic point (s_h), where it becomes zero. Transpiration is modeled as Eq. 1, being ET given by:

$$ET\left(s\right)=\begin{cases}0, & 0<s\leq s_h\\ E_w\frac{s-s_h}{s_w-s_h}, & s_h<s\leq s_w\\ E_w+\left(E_{max}-E_w\right)\frac{s-s_w}{s^*-s_w}, & s_w<s\leq s^*\\ E_{max}, & s^*<s\leq 1.\end{cases} \tag{10}$$

E_{max} is equal to $T_{max}+E_w$. AppendixB describes the modeling of the other variables in Eqs. 8 and 9.

Following Rodríguez-Iturbe et al. (1999) and Laio et al. (2001), the probability density function (pdf) of soil moisture under steady-state conditions may be derived from the Chapman-Kolmogorov forward equation. The general form of the solution is:

$$p\left(s\right)=\frac{C}{\rho\left(s,R_n\right)}\mathrm{e}^{-\gamma s+\lambda'\int\frac{du}{\rho(u)}},\ \text{for } s\geq s_h, \tag{11}$$

where λ' is the mean time between rainy days, and C is a constant that can be obtained by imposing the normalized condition $\int_{s_h}^{1}\rho\left(s\right)ds=1$. This constant is easily obtained numerically, although its analytical expressions are given in Laio et al. (2001) and Rodríguez-Iturbe and Porporato (2004). Details of the derivation of $p(s)$ can be found in Rodríguez-Iturbe and Porporato (2004); Laio et al. (2001); and Rodríguez-Iturbe et al. (1999). The general solution is:

$$p(s) = \begin{cases} \frac{C}{\eta_w}\left(\frac{s-s_h}{s_w-s_h}\right)^{T_1-1} \mathrm{e}^{-\gamma s} & s_h < s \leq s_w \\ \frac{C}{\eta_w}\left[1+\left(\frac{\eta}{\eta_w}-1\right)\frac{s-s_w}{s^*-s_w}\right]^{T_2-1} \mathrm{e}^{-\gamma s} & s_w < s \leq s_{cr} \\ \frac{C}{\eta}\mathrm{e}^{-\gamma s+\frac{\lambda'}{\eta}(s-s^*)}\left(\frac{\eta}{\eta_w}\right)^{T_2} & s_{cr} < s \leq s_{fc} \\ \frac{C}{\eta}\mathrm{e}^{-(\beta+\gamma)s+\beta s_{fc}}\left(\frac{\eta \mathrm{e}^{\beta s}}{(\eta-m)\mathrm{e}^{\beta s_{fc}}+m\mathrm{e}^{\beta s}}\right)^{T_3+1} & \\ \cdot\left(\frac{\eta}{\eta_w}\right)^{T_2-1}\mathrm{e}^{T_4} & s_{fc} < s \leq 1, \end{cases} \tag{12}$$

where

$$T_1 = \lambda' \tfrac{s_w-s_h}{\eta_w}, \qquad T_2 = \lambda' \tfrac{s^*-s_w}{\eta-\eta_w}, \qquad T_3 = \frac{\lambda'}{\beta(\eta-m)}, \qquad T_4 = \lambda' \frac{s_{fc}-s^*}{\eta}$$

$$\eta_w = \frac{E_w}{nZ_r}, \qquad \eta = \frac{E_{max}}{nZ_r}, \qquad m = \frac{K_s}{nZ_r\left[\mathrm{e}^{\beta\left(1-s_{fc}\right)}-1\right]}.$$

As mentioned before, the transpiration model of Laio et al. (2001) manages to describe the daily T dynamics in energy-limited ecosystems. Consequently, Eq. 10 manages to represent the evapotranspiration dynamics, and Eq. 12 the dynamics of soil moisture. This is proper as long as T_{max} (or E_{max}) is defined as a function of the available energy, and the stationarity of the parameters describing rainfall and radiation is preserved. It is noted that considerations in the model of Rodríguez-Iturbe et al. (1999) must continue to be taken into account, e.g., deep water table, soil homogeneity, distribution of infiltration volume into the rooting depth, etc. Interactions between vegetation and water table are not considered. This is a realistic assumption for water-controlled arid and semi-arid ecosystems, but may be a questionable one for energy-limited ecosystems. In the latter case, there may exist a close interaction between transpiration and the water table level (Tamea et al., 2009), but this may or not may impact heavily the pdf of soil moisture in systems that are both water- and energy-limited.

5. Daily dynamics

Fig. 3 shows the relationship between available energy and CO_2 assimilation, and available energy and the stomatal conductance in two sites,

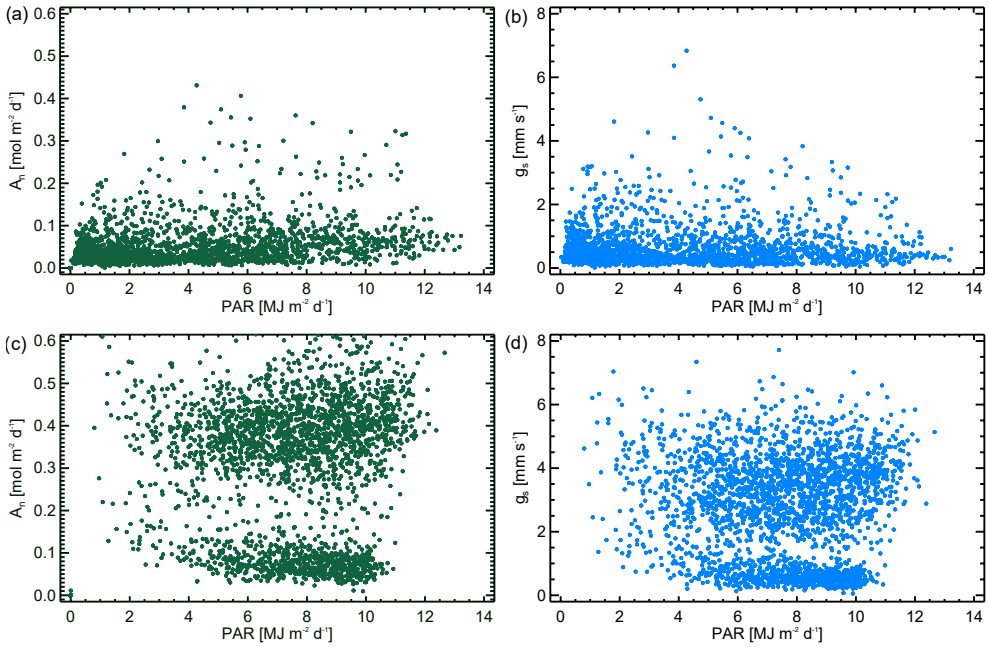

Figure 3: Relationship between daily PAR and CO_2 assimilation (left panel) and daily PAR and stomatal conductance (right panel) at (a,b) an extratropical site in Germany and (c,d) a tropical site in French Guiana.

one located in the extratropics (Germany) and other in the tropics (French Guiana). In the extratropics (Fig. 3(a,b)), the relationships of PAR and A_n, and PAR and g_s are positive for low values of PAR ($\approx$ 4 MJ m^2) and negative for high values. The photo-inhibition phenomenon, that occurs under strong light since it can destroy the plant tissues, can explain the above. This phenomenon involves the direct diversion of the superfluous radiation energy from the photosystems via fluorescence, and above as heat (Larcher, 1995). Nonetheless, at sites in tropics (see Fig. 3(c-d)), the relationships of PAR with g_s and A_n seem more random, which can be explained by the adaptation and the strategies developed by the plants at sites where they usually receive high radiation. We recalled that the PAR values analyzed correspond to those reaching the ground surface, and not those absorbed by the plant.

Fig. 4 shows the relationship between PAR and transpiration at the same sites in Fig. 3. In both types of ecosystems the relationship is direct since when PAR increases, both adiabatic and diabatic terms of Penman-Monteith increase. Radiation affects temperature, and this, in turn, modifies the vapor

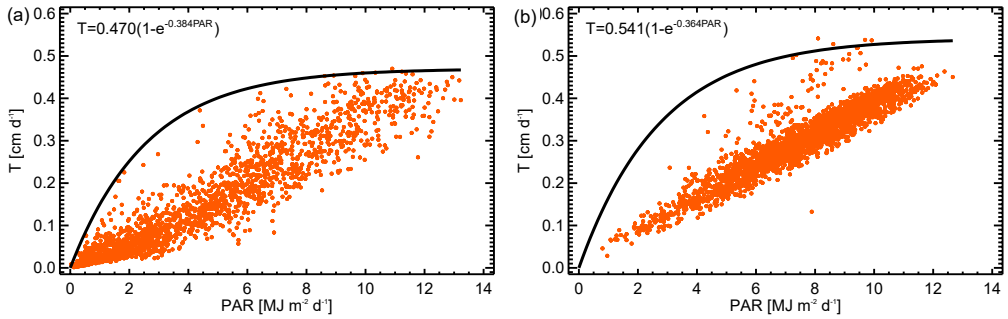

Figure 4: Relation of daily PAR and T in (a) an extratropical site and (b) a tropical site. The black line represents the proposed model to relate both variables.

saturation deficit. Furthermore, if there is available energy, the stomata open up as they can fix more CO_2, leading to the plant loses water. However, as shown in Fig. 3, the relation of PAR and g_s is not always direct, but g_s stabilizes (light-saturated plateau) at a point (Lambers et al., 2008), and may even decrease. The effect of light-saturation is also observed on T, but not that of the photo-inhibition, at least for the values of PAR measured at the sites studied.

Since transpiration is modeled using measured data, many factors may be limiting A_n, and consequently g_s and T, so a link between PAR and T must involve the envelope of simulated points relating these variables (see Fig. 4). For most sites, the envelope fits well to the expression:

$$T_{max}\left(PAR\right) = T^{*}\left(1 - \mathrm{e}^{-aPAR}\right). \tag{13}$$

This expression is a function of the maximum possible value of transpiration (light-saturation) (T^{*}) and a fitting parameter that determines the shape of the curve (a). This relationship avoids considering the indirect effects of radiation in transpiration (g_s, T_a, D, etc.). Fig. 4 shows the PAR-T curves (black lines) and their expressions in the sites in Germany and French Guiana. From Eq. 13 and considering the transpiration rate given by the vegetation physiology (T_{maxmax}), T_{max} can be defined as:

$$T_{max}\left(R\right) = \begin{cases} T^{*}\left(1 - \mathrm{e}^{-aR}\right), & T_{max}\left(R\right) < T_{maxmax} \\ T_{maxmax}, & T_{max}\left(R\right) \geq T_{maxmax}. \end{cases} \tag{14}$$

We noticed that available energy is considered as a constant since its stochasticity at the daily scale does not play a fundamental role in soil mois-

ture dynamics under the assumptions of theRodríguez-Iturbe et al. (1999) model, as shown by Muñoz (2019).

6. Analysis of sensitivity

Fig. 5 shows the response of soil water dynamics to PAR when other parameters of the Rodríguez-Iturbe et al. (1999) and Laio et al. (2001) model vary following the dimensionless groups:

$$\pi_1 = \frac{E_{max}}{\alpha\lambda}, \qquad \pi_2 = \frac{nZ_r}{\alpha}, \qquad \pi_3 = \frac{k_s}{\alpha\lambda}, \qquad \pi_4 = \frac{k_s}{E_{max}}. \tag{15}$$

These dimensionless groups are used because they simplify the interpretation and visualization of the results (Bridgman, 1922; Barenblatt, 1996; Gorokhovski and Hosseinipour, 1997; Butterfield, 1999; Barenblatt and Isaakovich, 2003). The sensitivity of the model output to each parameter is evaluated by moving the input parameter within an appropriate range and keeping the other parameters fixed. π_1 and π_2 groups have been adopted in previous works to analyze the soil moisture response to rainfall forcing, soil and vegetation changes (e.g. Li, 2014; Feng et al., 2012; Daly and Porporato, 2006; Porpotato et al., 2004; Rodríguez-Iturbe and Porporato, 2004; Guswa et al., 2002; Milly, 2001; Rodríguez-Iturbe et al., 1999; Milly, 1993).π_1 is the *dryness index* of Budyko (1974) and represents the ratio between the maximum evapotranspiration rate and the long-term mean rainfall rate. π_2 is called the *storage index* and is the ratio between the amount of water that can be stored in the soil (until the rooting depth) and the long-term mean rainfall depth (Feng et al., 2012). π_3 and π_4 are proposed by Guswa et al. (2002). π_3 is the *runoff index* and relates the saturated hydraulic conductivity coefficient and the long-term mean rainfall rate and, π_4 is the *infiltration index*, relating the saturated hydraulic conductivity and the maximum evapotranspiration rate.

For this analysis, we consider a loamy sand soil and a grass cover with the parameters in the caption of Fig. 5, where are the results of the four dimensionless groups are shown. In this, each color corresponds to a value of π, solid lines represent a low value of PAR (3 MJ m^{-2}), and dotted lines a high value (15 MJ m^{-2}). Fig. 5(a) shows the pdf of s ($f(s)$) for π_1 values between 0.1 and 1.4. As the value of π_1 increases, $f(s)$ moves to the left. Higher π_1 results in lower soil moisture values in the long-term, since the losses due to evapotranspiration are greater than soil water gains due to

rainfall. High values of available energy result in lower modes and greater dispersion than low PAR values. Fig. 5(b) shows $f(s)$ for π_2 varying between 4 and 20, since natural ecosystems tend to have root zones deep enough to result in values of π_2 larger than 1.0 (Milly, 2001). The higher the value of π_2, the lower the soil moisture. For large values of nZ_r, characteristic of plants with deeper roots such as trees, the amount of rainfall reaching the soil is distributed into a larger volume (according to the model), resulting in smaller increases in s. For lower values of nZ_r, rainfall is uniformly distributed in a smaller volume, increasing soil moisture rapidly. Very high and very low π_2 values occur when soil storage capacity is much larger or smaller than the rainfall amount, respectively. High PAR changes the dynamics of s, notably for high values of π related to large soil water storage or very small rainfall. Fig. 5(c) shows the results for π_3 values varying between 50 and 400. As the *runoff index* increases, the water moves rapidly out of the soil, decreasing s. As for π_2, the differences in available energy give very different dynamics of soil moisture for π_3, especially for high values of it, occurring when the amount of water flowing out the soil is much greater than the rainfall rate. Fig. 5(d) shows $f(s)$ for π_4 values between 100 and 1000. For low values of π_4, s remains high because water losses are minor. For high values of π_4 (greater than 550), the mode of the pdfs stabilizes near the field capacity point, changing only its frequency, and consequently, the dispersion. When k_s is much larger than E_{max}, soil loses water by leakage at a very high rate, being the evapotranspiration and its variability less relevant. High values of PAR result in curves more pulled to the left than low values of PAR.

If the available energy is high (dotted lines), the curves of $p(s)$ for all π groups move more rapidly to the left than when it is low (solid lines), since vegetation transpires at higher rates, maintaining soil moisture lower. The sensitivity of s is more noticeable for π values related to lower soil moisture because the demand of energy in the atmosphere changes the rate at which vegetation decreases its transpiration when it is under water stress. The dimensionless groups that consider E_{max} (π_1 and π_4) show less sensitivity to PAR and the modes always a minor frequency for high available energy. The other dimensionless groups (π_2 and π_3) show a more noticeable variation with PAR, completely changing the dynamics of s for some π values (e.g., π_2=16 and π_3=225). Furthermore, the mode has a high (low) frequency for low values of PAR when it is greater (lower) than s^*, decreasing (increasing) the dispersion.

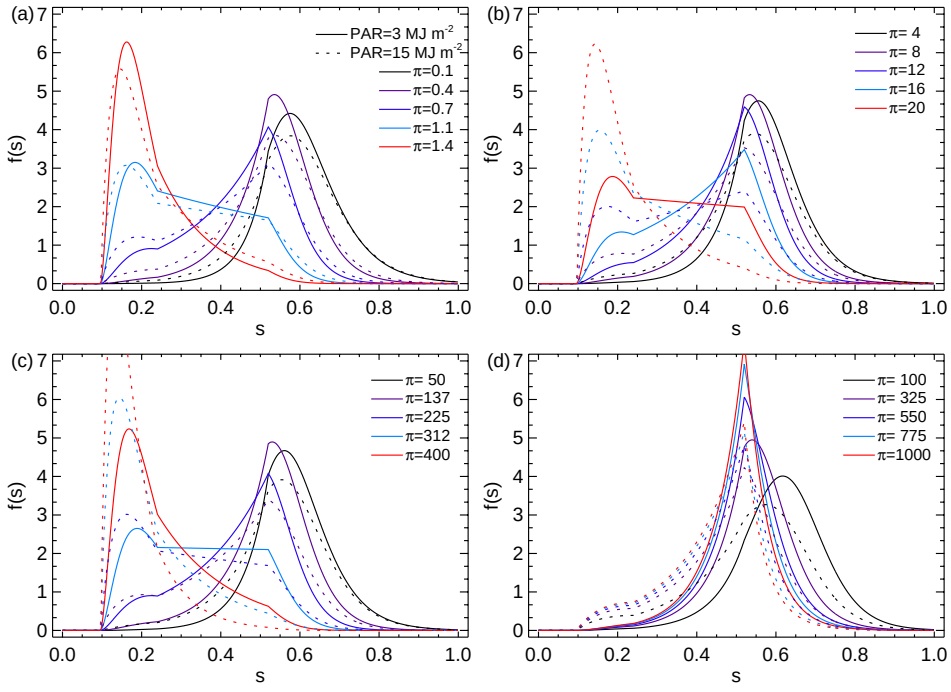

Figure 5: Dimensionless sensitivity analysis of soil water dynamics conditioned by available energy. Parameters in this figure are α=2 cm, λ=0.5 d^{-1}, Δ=0 cm, Z_r=30 cm, T_{max}=0.47 cm d^{-1}, a=0.384 m^2 MJ $^{-1}$, b=4.48, β=12.7, n=0.42, k_s=100 cm d^{-1}, s_h=0.08, s_w=0.10, s^*=0.24, and s_{fc}=0.52.

7. Water balance

Fig. 6 shows the behavior of the components of the water balance normalized by the average rainfall rate for a loamy sand soil. The expression of each component can be consulted in Laio et al. (2001) and Rodríguez-Iturbe and Porporato (2004). Figs. 6 (a,b) show the influence of rainfall events frequency (λ) for PAR equal to 3 and 15 MJ m^2, respectively. In both cases, the fraction of intercepted water (I) is constant and equal, since it changes in proportion to the rainfall rate. The percentage of runoff (Q) increases with λ in a similar proportion for both cases. The fraction of water transpired under stressed conditions (E_s) decreases rapidly until $\lambda \approx 0.3$ d^{-1} for PAR=3 MJ m^{-2} and until $\lambda \approx 0.5$ d^{-1} for PAR=15 MJ m^{-2}, being in the first case much lower. The same behavior is observed in the fraction of water transpired under non-stressed conditions (E_s). When PAR is low, the percentage of leakage is higher than when PAR is high, and the percentage of evapotranspired water is significantly lower. This suggests that more water reaching the soil is lost by evapotranspiration in water-limited regions than in energy-limited regions (for these parameter values), becoming Q and L more important in energy-limited ecosystems. These results are in agreement with field observations and results found in previous studies (e.g. Sala et al., 1992; Entekhabi and Rodríguez-Iturbe, 1994; Golubev et al., 2001; Rodríguez-Iturbe and Porporato, 2004; Robock and Li, 2006; Roderick et al., 2009).

Figs. 6(c,d) show the behavior of the water balance when λ and α are varied while maintaining constant the total amount of precipitation during a season Θ ($\Theta = \alpha \cdot \lambda \cdot nd$, being nd the number of days of the growing season) for PAR equal to 3 and 15 MJ m^2, respectively. For this figure $\Theta = 60$ cm and $nd = 200$ d. Interception increases almost linearly with λ while runoff decreases rapidly. According to Laio et al. (2001), this decreasing depends strongly on the ratio between soil depth and mean depth of rainfall events. The opposite behavior of interception and runoff determines a maximum of evapotranspiration at certain values of λ. As when only λ is varied, the main difference in the behavior of the water balance components for high and low PAR is observed in the percentage of evapotranspiration, being remarkably lower in the first case.

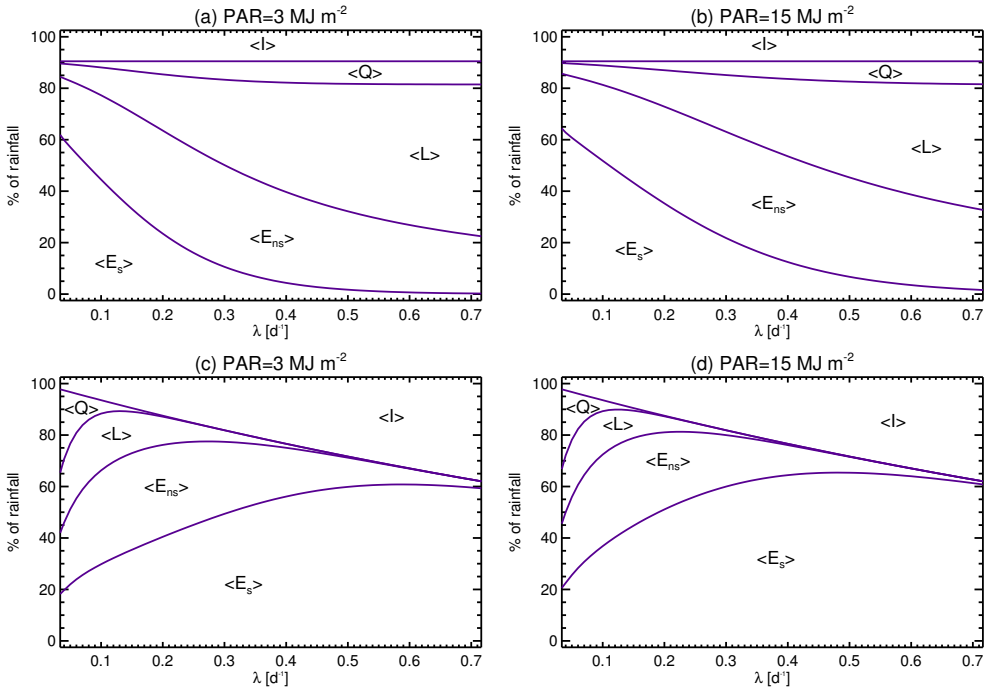

Figure 6: Examples of the behavior of the components of the water balance normalized by the total rainfall $\langle P \rangle$ for loamy sand soil, grass vegetation, and (a,c) PAR=3 MJ m^{-2} and (b,d) PAR=15 MJ m^{-2}. The parameters are shown in caption of Fig. 5.

8. Conclusions

In this paper, we have presented an analysis of transpiration as a function of available soil water and energy, extending the model of Rodríguez-Iturbe et al. (1999) and Laio et al. (2001), originally introduced to represent the pdf of soil moisture dynamics at a point in water-limited ecosystems, to the general case of ecosystems ranging from arid (water-limited) to humid (energy-limited). This model manages to describe the stochastic behavior of soil water content in environments limited by both energy and water, since evapotranspiration is expressed as a function of soil moisture and net radiation. This extension is valid as long as the E_{max} parameter is calculated taking into account the available energy, the parameters of both rainfall and radiation are stationarity, and considerations of the water-limited model are preserved, such as a deep water table, stationarity, homogeneous soil, and vegetation, etc.

We also analyzed the daily relationship of transpiration and photosynthetic active radiation by coupling the water and CO_2 fluxes through the leaf. As transpiration is directly related to the stomatal conductance, the relation between PAR and T is positive until a certain point where transpiration ceases to increase. We proposed an expression to parameterize the link between these two variables. This expression allows calculating the daily maximum transpiration rate from the value of daily available energy.

Several examples are presented exhibiting the influence of radiation on s, noticing that the available energy can notoriously change the soil moisture dynamics, and that evapotranspiration plays a more important role in water-limited than in energy-limited ecosystems. We note that these results are only valid on a daily scale since soil-climate-vegetation system dynamics change in more detailed temporal scales.

AppendixA. Assimilation model for C_3 plants

The photosynthesis rates limited by the Ribulose bisphosphate carboxylase-oxygenase (Rubisco) activity (A_c), and by the Ribulose bisphosphate (RuP_2) regeneration through electron transport (A_q) are given by:

$$A_c = V_{c,max}\left(T_l\right)\frac{c_i - \Gamma^*}{c_i + K_c\left(1 + o_i/K_o\right)}, \tag{A.1}$$

$$A_q = \frac{J}{4}\frac{c_i - \Gamma^*}{c_i - 2\Gamma^*}, \tag{A.2}$$

where Γ^* is the CO_2 compensation point (see Eq. 4), o_i is the intercellular oxygen concentration, $V_{c,max}$ is the maximum catalytic activity of Rubisco in the presence of saturating levels of RuP_2 and CO_2 (Eq. A.3), and K_c and K_o are Michaelis coefficients for CO_2 and O_2, respectively, given by Eq. A.4.

$$V_{c,max}\left(T_l\right) = V_{c,max_0}\frac{\exp\left[\frac{H_{vV}}{R_g T_0}\left(1-\frac{T_0}{T_l}\right)\right]}{1+\exp\left[\frac{S_v T_l - H_{dV}}{R_g T_l}\right]}, \tag{A.3}$$

$$K_x\left(T_l\right) = K_{x_0}\exp\left[\frac{H_{Kx}}{R_g T_0}\left(1-\frac{T_0}{T_l}\right)\right]. \tag{A.4}$$

J is the electron transport for a given absorbed photon irradiance, and is equal to $\min\left[J_{max}\left(T_l\right), Q\right]$, being J_{max} equal to:

$$J_{max}\left(T_l\right) = J_{max_0}\frac{\exp\left[\frac{H_{vJ}}{R_g T_0}\left(1-\frac{T_0}{T_l}\right)\right]}{1+\exp\left[\frac{S_v T_l - H_{dJ}}{R_g T_l}\right]}. \tag{A.5}$$

The parameters not mentioned here are described in Table 2.

AppendixB. Soil moisture model

The variables involved in Eq. 7, except the evapotranspiration (see Eq. 10 in section 4), are modeled as Rodríguez-Iturbe et al. (1999) and Laio et al. (2001).

AppendixB.1. Rainfall and interception

Daily precipitation is modeled through a marked Poisson process with arrival rate λ (Eagleson, 1972). The pdf of time intervals between rainy days τ is exponential with mean λ^{-1}:

$$f_T\left(\tau\right) = \lambda \mathrm{e}^{-\lambda\tau}, \text{ for } \tau \geq 0. \tag{B.1}$$

The marks correspond to the rainfall depth of rainy days, h, modeled as an independent exponentially distributed random variable with mean α

$$f_H\left(h\right) = \frac{1}{\alpha}\mathrm{e}^{-\frac{1}{\alpha}h}, \text{ for } h \geq 0. \tag{B.2}$$

The values of α and λ are assumed to be time-invariant quantities during the modeling period (growing season or climate season), i.e. rainfall is considered as a stationary stochastic process.

Rainfall rate is linked to the probability distributions expressed by Eqs. B.1 and B.2 as the marked Poisson process (Rodríguez-Iturbe and Porporato, 2004):

$$P(t) = \sum_{1} h_i \delta(t - t_i), \tag{B.3}$$

where $\delta(\cdot)$ is the Dirac delta function, h_i is the sequence of random rainfall depths distributed as eqn. B.2 and $[\tau_i = t_i - t_{i-1}, i = 1, 2, 3...]$ is the interarrival time sequence of a stationary Poisson process of frequency λ.

Following Rodríguez-Iturbe et al. (1999), interception is modeled through a threshold, Δ, such that only rainfall above Δ reaches the soil. The censored rainfall process is thus Poissonian with rate λ':

$$\lambda' = \lambda \int_{\Delta}^{\infty} f_H(h)\, dh = \lambda e^{-\frac{\Delta}{\alpha}}. \tag{B.4}$$

The depths h' of the censored rainfall process have the same exponential distribution as the original marks h (Rodríguez-Iturbe et al., 1999). Then, the new Poisson process is:

$$P(t) - I(t) = \sum_{1} h'_i \delta(t - t'_i), \tag{B.5}$$

where $\left[\tau'_i = t'_i - t'_{i-1}, i = 1, 2, 3...\right]$ is the interarrival time sequence of a stationary Poisson process with frequency λ'.

AppendixB.2. Infiltration and runoff

Surface runoff is generated via saturation excess (Dunne mechanism) that occurs when the infiltrated water saturates the soil profile. When rainfall depth is less than or equal to the available soil water storage, all the water from rainfall infiltrates. Infiltration is thus a function of the amount of rainfall and soil moisture, being a stochastic and state-dependent component. Its magnitude and temporal occurrence are controlled by soil moisture dynamics (Rodríguez-Iturbe and Porporato, 2004). The probability distribution of the infiltration may then be written as (Rodríguez-Iturbe et al., 1999):

$$f_Y(y,s) = \gamma e^{-\gamma y} + \delta(y-1-s)\int_{1-s}^{\infty} \gamma e^{-\gamma u} du, \text{ for } 0 \le y \le 1-s, \tag{B.6}$$

where $\gamma = \frac{nZ_r}{\alpha}$ and y is the dimensionless infiltration normalized by nZ_r. Infiltration from rainfall can be written as:

$$\varphi[s(t), t] = nZ_r \sum_{1} y_i \delta(t - t_i'), \tag{B.7}$$

where $[y_i, i = 1, 2, 3, ...]$ is the sequence of random infiltration events whose distribution is represented by Eq. B.6.

AppendixB.3. Leakage

Losses by leakage or deep infiltration, L, occur when soil water content is higher than field capacity, s_{fc}. The maximum percolation rate equals the saturated hydraulic conductivity, K_s, and decreases rapidly when the soil begins to dry, as expressed by (Laio et al., 2001):

$$L(s) = K(s) = \frac{K_s}{e^{\beta(1-s_{fc})} - 1}\left[e^{\beta(s-s_{fc})} - 1\right], \text{ for } s_{fc} < s \le 1. \tag{B.8}$$

AppendixB.4. Soil-drying process

During no-rain periods, soil moisture decays are deterministically modeled from initial values that depend on the the previous history of the entire soil-drying-wetting process. The soil moisture losses normalized by nZ_r are:

$$\begin{aligned} \rho(s, R_n) &= \frac{\chi(s, R_n)}{nZ_r} = \frac{E(s, R_n) + L(s)}{nZ_r} \\ &= \begin{cases} 0, & 0 < s \le s_h \\ \eta_w \frac{s - s_h}{s_w - s_h}, & s_h < s \le s_w \\ \eta_w + (\eta - \eta_w)\frac{s - s_w}{s^* - s_w}, & s_w < s \le s^* \\ \eta, & s^* < s \le s_{fc} \\ \eta + m\left[e^{\beta(s-s_{fc})} - 1\right], & s_{fc} < s \le 1. \end{cases} \end{aligned} \tag{B.9}$$

References

Albertson, J.D., Montaldo, N., 2003. Temporal dynamics of soil moisture variability: 1. Theoretical basis. Water Resources Research 39, 1274. doi:10.1029/2002WR001616.

Asbjornsen, H., Goldsmith, G.R., Alvarado-Barrientos, M.S., Rebel, K., Van Osch, F.P., Rietkerk, M., Chen, J., Gotsch, S., Tobon, C., Geissert, D.R., Gomez-Tagle, A., Vache, K., Dawson, T.E., 2011. Ecohydrological advances and applications in plant-water relations research: a review. Journal of Plant Ecology 4, 3–22. doi:10.1093/jpe/rtr005.

Baldocchi, D., Collineau, S., 1994. The Physical Nature of Solar Radiation in Heterogeneous Canopies: Spatial and Temporal Attributes, in: Caldwell, M., Pearcy, R. (Eds.), Exploitation of Environmental Heterogeneity by Plants. Academic Press. chapter 2, pp. 21–71.

Baldocchi, D., Falge, E., Gu, L., Olson, R., Hollinger, D., Running, S., Anthoni, P., Bernhofer, C., Davis, K., Evans, R., Fuentes, J., Goldstein, A., Katul, G., Law, B., Lee, X., Malhi, Y., Meyers, T., Munger, W., Oechel, W., Paw, K.T., Pilegaard, K., Schmid, H.P., Valentini, R., Verma, S., Vesala, T., Wilson, K., Wofsy, S., 2001. FLUXNET: A New Tool to Study the Temporal and Spatial Variability of Ecosystem–Scale Carbon Dioxide, Water Vapor, and Energy Flux Densities. Bulletin of the American Meteorological Society 82, 2415–2434. doi:10.1175/1520-0477(2001)082<2415:FANTTS>2.3.CO;2.

Baldocchi, D.D., Meyers, T.P., 1991. Trace gas exchange above the floor of a deciduous forest: 1. Evaporation and CO2 Efflux. Journal of Geophysical Research 96, 7271–7285.

Ball, J.T., Woodrow, I.E., Berry, J.A., 1987. A Model Predicting Stomatal Conductance and its Contribution to the Control of Photosynthesis under Different Environmental Conditions, in: Progress in Photosynthesis Research. Springer Netherlands, Dordrecht. chapter IV, pp. 221–224. doi:10.1007/978-94-017-0519-6-48.

Ballaré, C., 1994. Light Gaps: Sensing the Light Opportunities in Highly Dynamic Canopy Environments, in: Caldwell, M., Pearcy, R. (Eds.), Exploitation of Environmental Heterogeneity by Plants Environmental Heterogeneity by Plants. Academic Press. chapter 3, pp. 73–110.

Barenblatt, Isaakovich, G., 2003. Scaling. Cambridge University Press.

Barenblatt, G.I., 1996. Scaling, Self-similarity, and Intermediate Asymptotics: Dimensional Analysis and Intermediate Asymptotics. Cambridge University Press.

Bartlett, M.S., Vico, G., Porporato, A., 2014. Coupled carbon and water fluxes in CAM photosynthesis: modeling quantification of water use efficiency and productivity. Plant and Soil 383, 111–2138. doi:10.1007/s11104-014-2064-2.

Birmingham, B.C., Colman, B., 1979. Measurement of Carbon Dioxide Compensation Points of Freshwater Algae. Plant Physiology 64, 892–895. doi:10.1104/pp.64.5.892.

Bridgman, P.W., 1922. Dimensional analysis. Oxford University Press, United States of America.

Brooks, A., Farquhar, G.D., 1985. Effect of temperature on the CO2/O2 specificity of ribulose-1,5-bisphosphate carboxylase/oxygenase and the rate of respiration in the light. Planta 165, 397–406. doi:10.1007/bf00392238.

Brubaker, K.L., 1995. Nonlinear Dynamics of Water and Energy Balance in Land-Atmosphere Interaction. Ph.D. thesis. Massachusetts Institute of Technology. URL: http://dspace.mit.edu/handle/1721.1/36513{#}files-area.

Brubaker, K.L., Entekhabi, D., 1996. Analysis of feedback mechanisms in land-atmosphere interaction. Water Resources Research 32, 1343–1357.

Budyko, M., 1974. Climate and Life. Academic Press , 507.

Butterfield, R., 1999. Dimensional analysis for geotechnical engineers. Géotechnique 49, 357–366. doi:10.1680/geot.1999.49.3.357.

Chaves, M.M., Maroco, J.P., Pereira, J.S., 2003. Understanding plant responses to drought - From genes to the whole plant. Functional Plant Biology 30, 239–264. doi:10.1071/FP02076.

Chen, Z., Mohanty, B.P., Rodríguez-Iturbe, I., 2017. Space-time modeling of soil moisture. Advances in Water Resources 109, 343–354.

URL: https://doi.org/10.1016/j.advwatres.2017.09.009, doi:10.1016/j.advwatres.2017.09.009.

Collatz, G.J., Ball, J.T., Grivet, C., Berry, J.A., 1991. Physiological and environmental regulation of stomatal conductance, photosynthesis and transpiration: a model that includes a laminar boundary layer. Agricultural and Forest Meteorology 54, 107–136. doi:10.1016/0168-1923(91)90002-8.

Cooke, J.R., De Baerdemaeker, J.G., Rand, R.H., Mang, H.A., 1976. A finite element shell analysis of guard cell deformations. Transactions of the ASAE 19, 1107–1121.

Cordova, J., Bras, R.L., 1981. Physically Based Probabilistic Models of Infiltration, Soil Moisture, and Actual Evapotranspiration. Water Resources Research 17, 93–106.

Cowan, I.R., Farquhar, G.D., 1977. Stomatal function in relation to leaf metabolism and environment. Symposia of the Society for Experimental Biology 31, 471–505. doi:0081-1386.

Daly, E., Porporato, A., 2005. A Review of Soil Moisture Dynamics: From Rainfall Infiltration to Ecosystem Response. Environmental Engineering Science 22, 9–24. doi:10.1089/ees.2005.22.9.

Daly, E., Porporato, A., 2006. Impact of hydroclimatic fluctuations on the soil water balance. Water Resources Research 42, 1–11. doi:10.1029/2005WR004606.

Daly, E., Porporato, A., Rodríguez-Iturbe, I., 2004. Coupled Dynamics of Photosynthesis, Transpiration, and Soil Water Balance. Part I: Upscaling from Hourly to Daily Level. Journal of Hydrometeorology 5, 546–558. doi:10.1175/1525-7541(2004)005<0546:CDOPTA>2.0.CO;2.

Davies, W.J., Mansfield, T.A., Hetherington, A.M., 1990. Sensing of soil water status and the regulation of plant growth and development. Plant, Cell and Environment 13, 709–719. doi:10.1111/j.1365-3040.1990.tb01085.x.

de Assunção, A.A., dos Santos Souza, T.E.M., de Souza, E.R., Montenegro, S.M.G.L., 2018. Temporal dynamics of soil moisture and rainfall erosivity

in a tropical volcanic archipelago. Journal of Hydrology 563, 737–749. doi:10.1016/j.jhydrol.2018.06.047.

De Michele, C., Vezzoli, R., Pavlopoulos, H., Scholes, R., 2008. A minimal model of soil water-vegetation interactions forced by stochastic rainfall in water-limited ecosystems. Ecological Modelling 212, 397–407.

De Pury, D.G., Farquhar, G.D., 1997. Simple scaling of photosynthesis from leaves to canopies without the errors of big-leaf models. Plant, Cell and Environment 20, 537–557. doi:10.1111/j.1365-3040.1997.00094.x.

Dewar, R.C., 2002. The Ball-Berry-Leuning and Tardieu-Davies stomatal models: Synthesis and extension within a spatially aggregated picture of guard cell function. Plant, Cell and Environment 25, 1383–1398. doi:10.1046/j.1365-3040.2002.00909.x.

D'Odorico, P., Porporato, A., 2004. Preferential states in soil moisture and climate dynamics. Proceedings of the National Academy of Sciences of the United States of America 101, 8848–8851. doi:10.1073/pnas.0401428101.

D'Odorico, P., Ridolfi, L., Porpotato, A., Rodríguez-Iturbe, I., 2000. Preferential states of seasonal soil moisture: The impact of climate fluctuations. Water Resources Research 36, 2209–2219. doi:10.1029/2000WR900103.

Drake, B.G., Read, M., 1981. Carbon Dioxide Assimilation, Photosynthetic Efficiency, and Respiration of a Chesapeake Bay Salt Marsh. The Journal of Ecology 69, 405–423. doi:10.2307/2259676.

Eagleson, P.S., 1972. Dynamics of flood frequency. Water Resources Management 8, 878–898. doi:10.1029/WR008i004p00878.

Eagleson, P.S., 1978. Climate, soil, and vegetation: 1. Introduction to water balance dynamics. Water Resources Research 14, 705–712. doi:10.1029/WR014i005p00705.

Eagleson, P.S., 1982. Ecological optimality in water-limited natural soil-vegetation systems: 1. Theory and hypothesis. Water Resources Research 18, 325–340. doi:10.1029/WR018i002p00325.

Entekhabi, D., Brubaker, K.L., 1995. An Analytic Approach to Modeling Land-Atmosphere Interaction: 2. Stochastic Formulation. Water Resources Research 31, 633–643. doi:10.1029/94WR01773.

Entekhabi, D., Rodríguez-Iturbe, I., 1994. Analytical framework for the characterization of the space-time variability of soil moisture. Advances in Water Resources 17, 35–45. doi:10.1016/0309-1708(94)90022-1.

Fang, B., Lakshmi, V., 2014. Soil moisture at watershed scale: Remote sensing techniques. Journal of Hydrology 516, 258–272. doi:10.1016/j.jhydrol.2013.12.008.

Farquhar, G.D., 1973. A study of the responses of stomata to perturbations of environment. Phd. The Australian National University.

Farquhar, G.D., 1989. Models of Integrated Photosynthesis of Cells and Leaves. Philosophical Transactions of the Royal Society B: Biological Sciences 323, 357–367. doi:10.1098/rstb.1989.0016.

Farquhar, G.D., von Caemmerer, S., Berry, J.A., 1980. A biochemical model of photosynthetic CO2 assimilation in leaves of C3 species. planta 149, 78–90. doi:10.1007/BF00386231.

Feddes, R.A., Hoff, H., Bruen, M., Dawson, T., De Rosnay, P., Dirmeyer, P., Jackson, R.B., Kabat, P., Kleidon, A., Lilly, A., Pitman, A.J., 2001. Modeling root water uptake in hydrological and climate models. Bulletin of the American Meteorological Society 82, 2797–2809. doi:10.1175/1520-0477(2001)082<2797:MRWUIH>2.3.CO;2.

Feng, X., Vico, G., Porporato, A., 2012. On the effects of seasonality on soil water balance and plant growth. Water Resources Research 48, W05543. doi:10.1029/2011WR011263.

Fisher, J.B., Malhi, Y., Bonal, D., Da Rocha, H.R., De Araújo, A.C., Gamo, M., Goulden, M.L., Rano, T.H., Huete, A.R., Kondo, H., Kumagai, T., Loescher, H.W., Miller, S., Nobre, A.D., Nouvellon, Y., Oberbauer, S.F., Panuthai, S., Roupsard, O., Saleska, S., Tanaka, K., Tanaka, N., Tu, K.P., Von Randow, C., 2009. The land-atmosphere water flux in the tropics. Global Change Biology 15, 2694–2714. doi:10.1111/j.1365-2486.2008.01813.x.

Flexas, J., Medrano, H., 2002. Drought-inhibition of photosynthesis in C3 plants: Stomatal and non-stomatal limitations revisited. Annals of Botany 89, 183–189. doi:10.1093/aob/mcf027.

Gao, Q., Zhao, P., Zeng, X., Cai, X., Shen, W., 2002. A model of stomatal conductance to quantify the relationship between leaf transpiration, microclimate and soil water stress. Plant, Cell and Environment 25, 1373–1381.

Ge, S., Smith, R.G., Jacovides, C.P., Kramer, M.G., Carruthers, R.I., 2011. Dynamics of photosynthetic photon flux density (PPFD) and estimates in coastal northern California. Theoretical and Applied Climatology 105, 107–118.

Gevaert, A.I., Miralles, D.G., de Jeu, R.A.M., Schellekens, J., Dolman, A.J., 2018. Soil Moisture-Temperature Coupling in a Set of Land Surface Models. Journal of Geophysical Research: Atmospheres 3, 1481–1498. doi:10.1002/2017JD027346.

Golubev, S., Lawrimore, H., Groisman, Y., Speranskaya, A., Zhuravin, A., Menne, J., Peterson, C., Malone, W., 2001. Evaporation changes over the contiguous United States and the former USSR: A reassessment. Geophysical Research Letters 28, 2665–2668.

Gorokhovski, V., Hosseinipour, E.Z., 1997. Dimensionless Sensitivity Analysis of Subsurface Flow and Transport Models. Environmental & Engineering Geoscience III, 269–275. doi:10.2113/gseegeosci.III.2.269.

Guswa, A.J., Celia, M.a., Rodríguez-Iturbe, I., 2002. Models of soil moisture dynamics in ecohydrology: A comparative study. Water Resources Research 38, 5–1–5–15. doi:10.1029/2001WR000826.

Hansen, J.W., 1999. Stochastic daily solar irradiance for biological modeling applications. Agricultural and Forest Meteorology 94, 53–63. doi:10.1016/S0168-1923(99)00003-9.

Hosking, J., Clarke, R.T., 1990. Rainfall-Runoff Relations Derived From the Probability Theory of Storage. Water Resources Research 26, 1455–1463.

Jarvis, P.G., 1976. The Interpretation of the Variations in Leaf Water Potential and Stomatal Conductance Found in Canopies in the Field. Philosophical Transactions of the Royal Society B: Biological Sciences 273, 593–610. doi:10.1098/rstb.1976.0035.

772 Kattge, J., Knorr, W., 2007. Temperature acclimation in a biochemical model
773 of photosynthesis: A reanalysis of data from 36 species. Plant, Cell and
774 Environment 30, 1176–1190. doi:10.1111/j.1365-3040.2007.01690.x.

775 Kaufmann, M.R., 1976. Stomatal response of engelmann spruce to humidity,
776 light, and water stress. Plant physiology 57, 898–901. doi:10.1104/pp.
777 57.6.898.

778 Kim, G., Barros, A.P., 2002. Space-time characterization of soil moisture
779 from passive microwave remotely sensed imagery and ancillary data. Re-
780 mote Sensing of Environment 81, 393–403. doi:10.1016/S0034-4257(02)
781 00014-7.

782 Korres, W., Reichenau, T.G., Fiener, P., Koyama, C.N., Bogena, H.R., Cor-
783 nelissen, T., Baatz, R., Herbst, M., Diekkrüger, B., Vereecken, H., Schnei-
784 der, K., 2015. Spatio-temporal soil moisture patterns - A meta-analysis
785 using plot to catchment scale data. Journal of Hydrology 520, 326–341.
786 doi:10.1016/j.jhydrol.2014.11.042.

787 Laio, F., Porporato, A., Ridolfi, L., Rodríguez-Iturbe, I., 2001. Plants in
788 water-controlled ecosystems: Active role in hydrologic processes and re-
789 sponse to water stress: II. Probabilistic soil moisture dynamics. Advances
790 in Water Resources 24, 707–723. doi:10.1016/S0309-1708(01)00005-7.

791 Laio, F., Porporato, A., Ridolfi, L., Rodríguez-iturbe, I., 2002. On the sea-
792 sonal dynamics of mean soil moisture. Journal of Geophysical Research
793 107, ACL 8–1—-ACL 8–9.

794 Laio, F., Tamea, S., Ridolfi, L., D'Odorico, P., Rodriguez-Iturbe, I.,
795 Rodríguez-Iturbe, I., 2009. Ecohydrology of groundwater-dependent
796 ecosystems: 1. Stochastic water table dynamics. Water Resources Re-
797 search 45, 1–13. doi:10.1029/2008WR007292.

798 Lambers, H., Chapin, F.S., Pons, T.L., 2008. Plant Physiological Ecology.
799 Springer New York, New York, NY.

800 Larcher, W., 1995. Plant physiological ecology. Third ed., Springer Publish-
801 ers.

802 Legates, D.R., Mahmood, R., Levia, D.F., DeLiberty, T.L., Quiring, S.M.,
803 Houser, C., Nelson, F.E., 2011. Soil moisture: A central and unifying

theme in physical geography. Progress in Physical Geography 35, 65–86. doi:10.1177/0309133310386514.

Leuning, R., 1990. Modelling stomatal behaviour and and photosynthesis of Eucalyptus grandis. Functional Plant Biology 17, 159–175.

Leuning, R., 1995. A critical appraisal of combine stomatal model C3 plants. Plant, Cell & Environment 18, 339–355. doi:10.1111/j.1365-3040.1995.tb00370.x.

Leuning, R., Kelliher, F.M., De Pury, D.G.G., Schulze, E.D., 1995. Leaf nitrogen, photosynthesis, conductance and traspiration: scaling from leaves to canopies. Plant, Cell and Environment 18, 1183–1200.

Lhomme, J.P., 2001. Stomatal control of transpiration: Examination of the Jarvis-type representation of canopy resistance in relation to humidity. Water Resources Research 37, 689–699. doi:10.1029/2000WR900324.

Li, D., 2014. Assessing the impact of interannual variability of precipitation and potential evaporation on evapotranspiration. Advances in Water Resources 70, 1–11. doi:10.1016/j.advwatres.2014.04.012.

Luoma, S., 1997. Geographical pattern in photosynthetic light response of Pinus sylvestris in Europe. Functional Ecology 11, 273–281.

Manzoni, S., Katul, G., Fay, P.A., Polley, H.W., Porporato, A., 2011. Modeling the vegetation-atmosphere carbon dioxide and water vapor interactions along a controlled CO2 gradient. Ecological Modelling 222, 653–665. doi:10.1016/j.ecolmodel.2010.10.016.

Margulis, S.A., Entekhabi, D., 2001. A Coupled Land Surface-Boundary Layer Model and Its Adjoint. Journal of Hydrometeorology 2, 274–296. doi:10.1175/1525-7541(2001)002<0274:ACLSBL>2.0.CO;2.

Medlyn, B.E., De Kauwe, M.G., Lin, Y.S., Knauer, J., Duursma, R.A., Williams, C.A., Arneth, A., Clement, R., Isaac, P., Limousin, J.M., Linderson, M.L., Meir, P., Martin-Stpaul, N., Wingate, L., 2017. How do leaf and ecosystem measures of water-use efficiency compare? New Phytologist 246, 758–770. doi:10.1111/nph.14626.

Mielke, M.S., Oliva, M.A., De Barros, N.F., Penchel, R.M., Martinez, C.A., De Almeida, A.C., 1999. Stomatal control of transpiration in the canopy of a clonal Eucalyptus grandis plantation. Trees - Structure and Function 13, 152–160. doi:10.1007/s004680050199.

Milly, P.C.D., 1993. An analytic solution of the stochastic storage problem applicable to soil water. Water Resources Research 29, 3755–3758. doi:10.1029/93WR01934.

Milly, P.C.D., 2001. A minimalist probabilistic description of root zone soil water. Water Resources Research 37, 457–463. doi:10.1029/2000WR900337.

Miner, G.L., Bauerle, W.L., Baldocchi, D.D., 2017. Estimating the sensitivity of stomatal conductance to photosynthesis: a review. Plant Cell and Environment 40, 1214–1238. doi:10.1111/pce.12871.

Monteith, J., Unsworth, M., 2013. Principles of environmental physics: plants, animals, and the atmosphere. 4th edition ed., Academic Press.

Monteith, J.L., 1965. Evaporation and environment, in: Symposia of the Society for Experimental Biology, pp. 205–234.

Monteith, J.L., 1995. A reinterpritation of stomatal responses to humidity. Plant, Cell and Environment 18, 357–364.

Mtundu, N.D., Koch, R.W., 1987. A stochastic differential equation approach to soil moisture. Stochastic Hydrology and Hydraulics 1, 101–116. doi:10.1007/BF01543806.

Muñoz, E., 2019. Soil moisture dynamics in water- and energy-limited ecosystems . Application to slope stability. Phd. Universidad Nacional de Colombia.

Niemann, J., 2004. Scaling Properties and Spatial Interpolation of Soil Moisture. Technical Report. Pennsylvania State University, Department of Civil and Environmental Engineering. University Park, PA, USA. URL: http://oai.dtic.mil/oai/oai?verb=getRecord{&}metadataPrefix=html{&}identifier=ADA426497.

Noh, S.J., An, H., Kim, S., Kim, H., 2015. Simulation of soil moisture on a hillslope using multiple hydrologic models in comparison to field measurements. Journal of Hydrology 523, 342–355. doi:10.1016/j.jhydrol.2015.01.047.

Ogren, E., 1993. Convexity of the Photosynthetic Light-Response Curve in Relation to Intensity and Direction of Light during Growth. Plant physiology 101, 1013–1019. doi:10.1104/pp.101.3.1013.

Olson, R., Holladay, S., Cook, R., Falge, E., Baldocchi, D., Gu, L., 2004. FLUXNET. Database of fluxes, site characteristics, and flux-community information. Technical Report. Oak Ridge National Laboratory (ORNL). Oak Ridge, TN (United States). URL: http://www.osti.gov/servlets/purl/1184413/, doi:10.2172/1184413.

Pallardy, S.G., 2008. Transpiration and Plant Water Balance, in: Physiology of Woody Plants. Elsevier, pp. 325–366.

Peters-Lidard, C.D., Zion, M.S., Wood, E.F., 1997. A soil-vegetation-atmosphere transfer scheme for modeling spatially variable water and energy balance processes. Journal of Geophysical Research: Atmospheres 102, 4303–4324. doi:10.1029/96JD02948.

Petersen, K.L., Moreshet, S., Fuchs, M., 1991. Stomatal Responses of Field-Grown Cotton to Radiation and Soil Moisture. Agronomy Journal 83, 1059. doi:10.2134/agronj1991.00021962008300060024x.

Petersen, K.L., Moreshet, S., Fuchs, M., Schwartz, A., 1992. Field cotton stomatal responses to light spectral composition and variable soil moisture. European Journal of Agronomy 1, 117–123 ST – Field cotton stomatal responses to l. doi:10.1016/S1161-0301(14)80009-9.

Pieruschka, R., Huber, G., Berry, J.A., 2010. Control of transpiration by radiation. Proceedings of the National Academy of Sciences 107, 13372–13377. doi:10.1073/pnas.0913177107.

Pirone, M., Papa, R., Nicotera, M.V., Urciuoli, G., 2015. Soil water balance in an unsaturated pyroclastic slope for evaluation of soil hydraulic behaviour and boundary conditions. Journal of Hydrology 528, 63–83. doi:10.1016/j.jhydrol.2015.06.005.

Porporato, A., Laio, F., Ridolfi, L., 2003. Soil moisture and plant stress dynamics along the Kalahari precipitation gradient. Journal of Geophysical Research 108, 1–8. doi:10.1029/2002JD002448.

Porporato, A., Rodríguez-iturbe, I., 2002. Ecohydrology-a challenging multidisciplinary research perspective. Hydrological Sciences Journal 47, 811–821.

Porpotato, A., Daly, E., Rodríguez-Iturbe, I., 2004. Soil Water Balance and Ecosystem Response to Climate Change. The American Naturalist 164, 627–632. doi:10.1086/676943.

Ridolfi, L., D'Odorico, P., Porporato, A., Rodríguez-Iturbe, I., Rodriguez-Iturbe, I., 2003. Stochastic soil moisture dynamics along a hillslope. Journal of Hydrology 272, 264–275. doi:10.1016/S0022-1694(02)00270-6.

Rigon, R., Bertoldi, G., Over, T.M., 2006. GEOtop: A Distributed Hydrological Model with Coupled Water and Energy Budgets. Journal of Hydrometeorology 7, 371–388. doi:10.1175/JHM497.1.

Robock, A., Li, H., 2006. Solar dimming and CO_2 effects on soil moisture trends. Geophysical Research Letters 33, 1–5. doi:10.1029/2006GL027585.

Roderick, M.L., Hobbins, M.T., Farquhar, G.D., 2009. Pan evaporation trends and the terrestrial water balance. II. Energy balance and interpretation. Geography Compass 3, 761–780. doi:10.1111/j.1749-8198.2008.00214.x.

Rodríguez-Iturbe, I., Porporato, A., 2004. Ecohydrology of Water-Controlled Ecosystems. Cambridge University Press, USA.

Rodriguez-Iturbe, I., Porporato, A., Laio, F., Ridolfi, L., 2001. Plants in water-controlled ecosystems: active role in hydrologic processes and response to water stress I. Scope and general outline. Advances in Water Resources 24, 725–744. doi:10.1016/S0309-1708(01)00006-9.

Rodríguez-Iturbe, I., Porporato, A., Ridolfi, L., Isham, V., Coxi, D., 1999. Probabilistic modelling of water balance at a point: the role of climate, soil and vegetation. Proceedings of the Royal Society A: Mathematical, Physical and Engineering Sciences 455, 3789–3805. doi:10.1098/rspa.1999.0477.

928 Sala, O.E., Lauenroth, W.K., Parton, W.J., 1992. Long-term soil water
929 dynamics in the shortgrass steppe. Ecology 73, 1175–1181. doi:10.2307/
930 1940667.

931 Schulze, E.D., 1986. Whole-Plant Responses to Drought. Functional Plant
932 Biology 13, 127–141.

933 Schulze, E.D., Leuning, R., Kelliher, F.M., 1995. Environmental regulation
934 of surface conductance for evaporation from vegetation. Vegetatio 121,
935 79–87. doi:10.1007/BF00044674.

936 Sela, S., Svoray, T., Assouline, S., 2012. Soil water content variability at the
937 hillslope scale: Impact of surface sealing. Water Resources Research 48,
938 W03522. doi:10.1029/2011WR011297.

939 Seneviratne, S.I., Corti, T., Davin, E.L., Hirschi, M., Jaeger, E.B., Lehner,
940 I., Orlowsky, B., Teuling, A.J., 2010. Investigating soil moisture-climate
941 interactions in a changing climate: A review. Earth-Science Reviews 99,
942 125–161. doi:10.1016/j.earscirev.2010.02.004.

943 Shan, N., Ju, W., Migliavacca, M., Martini, D., Guanter, L., Chen, J.,
944 Goulas, Y., Zhang, Y., 2019. Modeling canopy conductance and transpira-
945 tion from solar-induced chlorophyll fluorescence. Agricultural and Forest
946 Meteorology 268, 189–201. doi:10.1016/j.agrformet.2019.01.031.

947 Stoy, P.C., Richardson, A.D., Baldocchi, D.D., Katul, G.G., Stanovick, J.,
948 Mahecha, M.D., Reichstein, M., Detto, M., Law, B.E., Wohlfahrt, G.,
949 Arriga, N., Campos, J., McCaughey, J.H., Montagnani, L., Paw U, K.T.,
950 Sevanto, S., Williams, M., 2009. Biosphere-atmosphere exchange of CO2
951 in relation to climate: A cross-biome analysis across multiple time scales.
952 Biogeosciences 6, 2297–2312. doi:10.5194/bg-6-2297-2009.

953 Tamea, S., Laio, F., Ridolfi, L., D'Odorico, P., Rodríguez-Iturbe, I., 2009.
954 Ecohydrology of groundwater-dependent ecosystems: 2. Stochastic soil
955 moisture dynamics. Water Resources Research 45, 1–13.

956 Tardieu, F., Simonneau, T., Muller, B., 2018. The Physiological Ba-
957 sis of Drought Tolerance in Crop Plants: A Scenario-Dependent Prob-
958 abilistic Approach. Annual Review of Plant Biology 69. doi:10.1146/
959 annurev-arplant-042817-040218.

960 Thorpe, M.R., Saugier, B., Auger, S., Berger, A., Methy, M., 1978. Pho-
961 tosynthesis and transpiration of an isolated tree: model and validation.
962 Plant, Cell and Environment 1, 269–277.

963 Tuzet, A., Perrier, A., Leuning, R., 2003. A coupled model of stomatal con-
964 ductance, photosynthesis and transpiration. Plant, Cell and Environment
965 26, 1097–1116. doi:10.1046/j.1365-3040.2003.01035.x.

966 Wagner, W., Lemoine, G., Rott, H., 1999. A method for estimating soil
967 moisture from ERS scatterometer and soil data. Remote Sensing of Envi-
968 ronment 70, 191–207.

969 Wang, C., Fu, B., Zhang, L., Xu, Z., 2019. Soil moisture-plant interactions:
970 an ecohydrological review. Journal of Soils and Sediments 19. doi:10.
971 1007/s11368-018-2167-0.

972 Xu, Z., Zhou, G., Shimizu, H., 2010. Plant responses to drought and rewa-
973 tering. Plant Signaling and Behavior 5, 649–654. doi:10.4161/psb.5.6.
974 11398.

975 Yu, Q., Zhang, Y., Liu, Y., Shi, P., 2004. Simulation of the Stomatal Con-
976 ductance of Winter Wheat in Response to Light, Temperature and CO2
977 Changes. Annals of Botany 93, 435–441. doi:10.1093/aob/mch023.

978 Zehe, E., Loritz, R., Jackisch, C., Westhoff, M., Kleidon, A., Blume, T.,
979 Hassler, S., Savenije, H.H., 2018. Energy states of soil water - a ther-
980 modynamic perspective on storage dynamics and the underlying con-
981 trols. Hydrology and Earth System Sciences Discussions 23, 971–978.
982 doi:10.5194/hess-2018-346.

983 Zhang, K., Kimball, J.S., Running, S.W., 2016. A review of remote sens-
984 ing based actual evapotranspiration estimation. Wiley Interdisciplinary
985 Reviews: Water 3, 834–853. doi:10.1002/wat2.1168.